

Genesis and variation spatial of Podzol in depressions of the Barreiras formation, northeastern Espírito Santo State, Brazil, and its implications for Quaternary climate change

Article

Accepted Version

Creative Commons: Attribution-Noncommercial-No Derivative Works 4.0

Schiavo, J. A., Pessenda, L. C. R., Buso Junior, A. A., Calegari, M. R., Fornari, M., Secretti, M. L., Pereira, M. G. and Mayle, F. E. ORCID: https://orcid.org/0000-0001-9208-0519 (2020) Genesis and variation spatial of Podzol in depressions of the Barreiras formation, northeastern Espírito Santo State, Brazil, and its implications for Quaternary climate change. Journal of South American Earth Sciences, 98. 102435. ISSN 0895-9811 doi: 10.1016/j.jsames.2019.102435 Available at https://centaur.reading.ac.uk/87432/

It is advisable to refer to the publisher's version if you intend to cite from the work. See <u>Guidance on citing</u>.

To link to this article DOI: http://dx.doi.org/10.1016/j.jsames.2019.102435

Publisher: Elsevier



All outputs in CentAUR are protected by Intellectual Property Rights law, including copyright law. Copyright and IPR is retained by the creators or other copyright holders. Terms and conditions for use of this material are defined in the <u>End User Agreement</u>.

www.reading.ac.uk/centaur

CentAUR

Central Archive at the University of Reading

Reading's research outputs online

- 1 Genesis and variation spatial of Podzol in depressions of the Barreiras Formation,
- 2 northeastern Espírito Santo State, Brazil, and its implications for Quaternary climate
- 3 change.
- 4 Jolimar Antonio Schiavo^a, Luiz Carlos Ruiz Pessenda^b, Antonio Alvaro Buso Júnior^b, Marcia
- Regina Calegari^c, Mileni Fornari^b, Mateus Luiz Secretti^a; Marcos Gervasio Pereira^d; Frank
 Edward Mayle^e
- ^aUniversidade Estadual de Mato Grosso do Sul, Unidade Universitária de Aquidauana,
 Rodovia Aquidauana, km 12, Aquidauana, Mato Grosso do Sul, Brazil.
- ^bUniversidade de São Paulo, Laboratório de ¹⁴C, Avenida Centenário 303, 13400-970,
 Piracicaba, São Paulo, Brazil.
- ^cUniversidade Estadual do Oeste do Paraná, Campus Marechal Cândido Rondon, Colegiado
 de Geografia, Rua Pernambuco, 1777, CX Postal 91, CEP:85970-020, Mal. Cd Rondon,
 Paraná, Brazil.
- ^dUniversidade Federal Rural do Rio de Janeiro, Instituto de Agronomia, Departamento de
 Solos, BR-465, Seropédica, Rio de Janeiro, Brazil.
- ^eUniversity of Reading, Centre for Past Climate Change and Department of Geography &
 Environmental Science, Reading RG6 6DW, Berkshire, UK.
- ABSTRACT. Variations in relief associated with pedogenetic processes promote 18 different intensities in weathering of sediments of the Barreiras Formation and may thus lead 19 20 to the formation of different soil types, like Podzols, Acrisols and Ferralsols. The Podzols of tropical regions contain important information on climate and vegetation changes that 21 occurred mainly in late Pleistocene and Holocene; however few studied, regarding their 22 spatial variation, that can be investigated through ground penetrating radar (GPR). The aim 23 was to study morphological, physical, chemical, stable C isotopic properties and spatial 24 distribution of soils within depressions of the Barreiras Formation and characterize the ¹⁴C 25 chronology of two Podzols and their B spodic horizons, along a transect grassland to forest in 26 northeastern Espírito Santo State, Brazil. The profiles encompass a sequence of A-E-Bhm 27 horizons, except for P3 and P6 with histic H and A-Bt, respectively. The GPR images showed 28 patterns corresponding to these soil horizons, and the GPR data reveal the presence of 29

diagnostic subsurface horizons characteristic of spodic horizons with cemented layers. The 30 influence of relief factors and original materials was observed, associated with ferrolysis and 31 podzolisation as main actors in the genesis of soils studied. The monomorphic organic matter 32 33 filling the voids evidences the processes of imobilization, illuviation and precipitation, with the genesis of the spodic horizon. The Podzols profiles of Pleistocene organic matter ages 34 accumulated compounds of C₃ plants from the vegetation cover in the B spodic horizons of 35 36 the profiles P4 and P1, since at least 14,251 and 38,890 cal BP, respectively, suggesting the dominance of a humid climate at least during the studied period in the region. 37

38 Keywords: Ground penetrating radar, Organic matter, Stable carbon isotopes, ¹⁴C dating,
39 Micromorphology, Podzolisation.

40

1. Introduction

The north and northeastern regions of Espírito Santo State, Brazil, encompass the Tabuleiros Costeiros (coastal plains) geomorphological unit, which comprises sandy-clayey Tertiary deposits of the Barreiras Group. In this coastal plain, there are gentle depressions, which favor the lateral flow of water with installation of water table, forming types of soils different from those of the higher parts of the landscape (Pessenda et al., 2015; Calegari et al., 2017).

47 Ferralsols and Acrisols are predominant soils and occupy the highest parts of the landscape of this region and have been well studied (Moreau et al., 2006; Corrêa et al., 2008; 48 Lima Neto et al., 2009; Dantas et al., 2014), and are characterized by sandy loam to clay 49 texture, yellowish tones, low nutrient availability and cation exchange capacity, exchangeable 50 aluminum and aluminum saturation, and kaolinite mineralogy (Lima Neto et al., 2009). The 51 lower parts of the landscape are associated with sandy soils like Arenosols and Podzols. In the 52 coastal plains, the vegetation shows different physiognomies associated with markedly 53 different soil types, i.e., Ferralsols and Acrisols are associated with Lowland Tropical 54

Rainforest, while the Arenosols and Podzols are associated with the grasslands (Saporetti-Junior et al., 2012).

The Podzols have important environmental functions such as being a filter for pollutants and a sink for atmospheic carbon (Sauer et al., 2007; Montes et al., 2011; Lopes-Mazzetto et al., 2018), as well as representing areas with large numbers of endemic and niches specific species being designated as conservation areas (Buso Júnior et al., 2013, Mendonça et al., 2015).

Among the various theories proposed to explain the formation of Podzols (Anderson et al., 1982; Buurman and Jongmans, 2005; DeConinck, 1980; Lundstrom et al., 2000a), the complexation and transport of dissolved organic matter (DOM) with Fe and Al play an important role in the formation of the B spodic horizon. Typically, the B spodic horizon shows colors ranging from black to reddish brown, enriched by organic matter, Al and sometimes Fe.

The natural drainage conditions influence the formation of Podzols, mainly in the 68 morphology and distinction of horizons, in the accumulation and stabilization of organic 69 70 matter and Fe in the B spodic horizon. The presence or absence of Fe can be used as an indicator of drainage conditions. Poorly drained Podzols have lost all Fe due to reduction and 71 72 lateral removal, while in well-drained podzols Fe is still present, and intermediate drainage 73 conditions are recognised by Fe mottles (Buurman, 1984; DeConinck et al., 1974). In addition 74 to Fe, drainage conditions can cause variations in the morphology of Podzols as thickness of the B horizon and the shape of the EB transition, i.e. those poorly drained have flat EB 75 transition caused by the highest groundwater level; while the well-drained have a thin 76 undulating Bh horizon, dependent on the vertical movement of percolated water (Buurman et 77 al., 2005, 2013; Lopes-Mazzetto et al., 2018; Kaczorek et al., 2004; Schwartz, 1988). In 78 poorly drained podzols, the B horizon is water-saturated during large part of the year, and the 79

organic matter is predominantly DOM derived. In well-drained podzols, the B horizon may have a contribution from in situ root materials and the DOM has a very local source due to vertical movement of percolating water (Lopes-Mazzetto et al., 2018). More detailed studies of organic matter such as determination of the elemental composition by pyrolisis (Lopes-Mazzetto et al., 2018), ¹²C and ¹³C isotopic variation, ¹⁴C dating (Horbe et al., 2004) and Spodic B horizon micromorphology (Bardy et al., 2008; Coelho et al., 2012) may contribute to inferring the genesis of Podzols.

The podzols of tropical environments, such as those of coastal plain in Brazil, may be much older and consequently with greater variations of climate and vegetation (Boski et al., 2015; Martinez et al., 2018), when compared to Podzols of boreal and temperate areas with Holocene age with moderate variations in the climate.

In Brazil, detailed studies of the classification and genesis of Podzols have been made in
individual profiles (Mafra et al., 2002; Coelho et al., 2010b; Coelho et al., 2010c; Oliveira et
al., 2010; Schiavo et al., 2012; Carvalho et al., 2013), but little is known about the spatial
variation of the podzolisation process as a function of climate and vegetation.

95 Vale Nature Reserve (VNR) is a 28,000-hectare area of protected vegetation, located in the northeastern Espirito Santo State, in the municipality of Linhares, Brazil. The 96 97 vegetation shows different physiognomies associated with markedly different soil types. Soil variations across the landscape can be better understood in the context of micro-relief and 98 99 associated variations in vegetation type. The Tabuleiros forest (Lowland Tropical Rainforest) is the dominant matrix, occurring in the higher parts of the landscape, being associated with 100 Ferralsols and Acrisols (Moreau et al., 2006; Corrêa et al., 2008; Lima Neto et al., 2009; Silva 101 et al., 2013; Dantas et al., 2014). Mussununga vegetation occurs interspersed with the 102 Tabuleiros forest and varies from grasslands (campos nativos) to wooded savannah and 103 woodland (Saporetti-Junior et al., 2012) and it is associated with sandy soils such as 104

105 Arenosols and Podzols (Pessenda et al., 2015; Calegari et al., 2017; Buso Júnior et al., 2019). 106 In this region, these authors verified using distinct proxies (pollen, δ^{13} C, δ^{15} N, ¹⁴C dating and 107 phytoliths) that the Podzols genesis is related to changes in vegetation and climate, occurring 108 between the Holocene and late Pleistocene.

In this environment, the ground penetrating radar (GPR) is a tool that can contribute to the understanding of the spatial variation and arrangement (thickness, depth and transition) of the horizons of Podzols. According to the principle of GPR, the morphological differentiation between the horizons of the Podzols can be detected by the emission of different electromagnetic pulses (Ucha et al., 2010), and consequently, it can be inferred in the spatial distribution of these horizons.

The aim of the present study is to characterize the morphological, physical and chemical properties of soils (Podzol), associated with GPR data and stable C isotopes of the soil profile, across the ecotone between native grassland and Tabuleiro forest in northeastern Espírito Santo State, Brazil, in order to understand the genesis and spatial distribution of the B spodic horizon and its relation to vegetation and soil properties.

120 **2.** Study site

121 The study area is located in the Vale Nature Reserve (VNR), northeastern of the 122 Espírito Santo State, Brazil. The VRN is a protected area within the natural range of the 123 lowland Atlantic Forest, and it is one of the most important areas for biodiversity 124 conservation (Ministério do Meio Ambiente, 2000).

The geological landscape is characterized by highland areas with Precambrian rocks, offering an uneven relief occupied by Atlantic Forest, and a system of dendritic rivers. The Neogene plateau to the east of the relief, locally called Tabuleiros Costeiros, is formed by continental deposits of the Barreiras Formation (Tertiary period), a flat terrain with a corrugated slope towards the sea. The Tabuleiros comprises marine, fluvial-marine, lagoon and eolian sediments accumulated during the Quaternary. The Tabuleiros evolution was
strongly controlled by relative sea-level changes, fluvial sedimentation, long shore drift, and
changes in atmospheric circulation (Martin et al., 1993).

133

3. Material and methods

The soil sampling was carried out in the VNR (19°11'58" S and 40°05'22" W. Fig. 1). The climate in the region is warm and humid, tropical type (Aw), with a rainy season in the austral summer and dry winter, mean annual precipitation of 1215 mm, mean annual temperature of 23.3 °C (Buso Junior et al. 2013). In the area of the VNR, it is possible to distinguish (with a resolution of ~5.0 meters) distinct vegetation-soil relationships in circular areas of grasslands within Tabuleiro forest, with transitional shrub vegetation.

Six trenches were dug within two study areas spanning the center of the grassland to 140 the Tabuleiro forest: transect 1 – profile P1: 19⁰ 09' 11.30" S 40⁰ 03'55.40" W (grassland 141 mussununga), P2: 19⁰ 09'16.20" S 40⁰ 03' 54.80" W (shrubland mussununga), P3: 19⁰ 142 09'17.16" S 40⁰ 03'55.20" W (woodland mussununga); transect 2 – profile P4: 19⁰12'47.00" 143 S 39⁰ 57'52.00" W (grassland mussununga), P5: 19⁰12'36.10" S 39⁰ 57'40.80" W (shrubland 144 mussununga) and P6: 19⁰ 12'35.34" S 39⁰ 57'36.30" W (woodland mussununga). Inside the 145 trenches the profiles were morphologically described based on Santos et al. (2015), and 146 147 samples collected from all horizons. Disturbed soil samples were air-dried, ground and sieved (fraction < 2 mm) to be used for physical and chemical analyses as described in Teixeira et al. 148 (2017). The particle size was determined by the pipette method, using sodium hydroxide 0.1 149 mol L⁻¹ as dispersant. 150

To determine and map the soil horizons and assess spatial variations in soil properties, ground-penetrating radar (GPR) was used along 15 km, with transects across a representative soil area using the TerraSIR Subsurface Interface Radar (SIR) System-3000 (Geophysical Survey Systems, Inc., Salem, New Hampshire) with 200 MHz antenna (Fig. 1). The 200-MHz

frequency was chosen after in situ testing with a series of antenna frequencies (70 MHz, 400 155 MHz, 270 MHz and 200 MHz). The 200 MHz frequency provided the optimal balance of 156 image quality, detection depth, and the convenience of operation in the area with both 157 grassland and Tabuleiro forest. Traces along the GPR transects were adjusted vertically for 158 variations in topography, using a real time kinematic global positioning system. Data 159 processing included applying a zero time adjustment to find true ground surface reflection, 160 same gain factor, dewow filter, a tapered bandpass filter (20-40-300-600 MHz) and an 161 automatic gain control (AGC), using the RADAN for Windows[™] software program (version 162 7, GSSI). 163

The exchangeable cations Ca^{2+} , Mg^{2+} and Al^{3+} were extracted with 1mol L^{-1} KCl 164 solution, the H+Al with a 0.5 mol L⁻¹ calcium acetate solution with pH 7.0. For the extraction 165 of P, Na⁺ and K⁺ the solution of H₂SO₄ 0.0125 mol L⁻¹ + HCl 0.05 mol L⁻¹ was used. The 166 levels of Ca^{2+} and Mg^{2+} were determined by titrations with 0.0125 mol L⁻¹ EDTA solution; 167 Na⁺ and K by flame photometry; P by colorimetry; and Al³⁺ and H+ Al, by titrations with 168 NaOH 0.025 mol L⁻¹. The pH in water and KCl (weight 1:2.5) was determined by means of a 169 potentiometer. The content of total organic carbon (TOC) was determined according to 170 Yeomans and Bremner (1988). From these results, the following were calculated: the 171 172 saturation by aluminum (m); the SB value (sum of exchangeable bases); T value (CTC of the ground) and V value. All the above procedures were carried out according to Teixeira et al. 173 (2017). 174

The forms of Fe and Al, in their varying degrees of crystallinity, were evaluated by the use of sodium dithionite–citrate–bicarbonate (DCB) (Mehra and Jackson, 1960), and of acid ammonium oxalate (Ox), (Mckeague and Day, 1966), with determination of extracts by atomic absorption spectrometry.

The profiles P1 and P4, horizons Bhx1 (1.49-1.60 m) and Bhm1/Bhm2 (0.91-1.11 m) 179 respectively, were selected for ¹⁴C dating. These soil samples were treated according to 180 Pessenda et al. (1996) for humin extraction. Treatments included the removal of modern roots 181 fragments by handpicking, followed by the removal of fulvic and humic acids. The samples 182 were combusted at the ¹⁴C Laboratory and the purified CO₂ was sent to the LACUFF 183 Laboratory, Brazil for accelerator mass spectrometry (AMS) dating (Macario et al., 2013). 184 185 Ages are expressed as years before present (BP) and calibrated ages (cal. BP, 2σ), according to the SHCal13 curve (Hogg et al., 2013), using the software CALIB Rev 7.0.4 (Stuiver and 186 Reimer, 1993) for ¹⁴C age calibration. 187

In addition, in the profiles P1 and P4 (native grassland) soil samples were collected 188 each 10 cm for analysis of carbon stable isotopes (δ^{13} C). The profiles P1 and P4 were 189 collected up to 1.8 m and 3.70 m, respectively. Modern root fragments were manually 190 removed from soil samples selected for C analyses and sieved (350 µm) with distilled water to 191 remove coarse sand grains. All samples were dried at 50 °C. Analyses were carried out at the 192 Stable Isotope Laboratory (CENA/USP) using an elemental analyzer attached to an ANCA 193 SL 2020 mass spectrometer. Stable isotopes (δ^{13} C) were measured with respect to VPDB as 194 standard and are expressed as *per mil* (‰) with a standard deviation of 0.2‰. 195

The natural oriented samples taken for micromorphological analyses were collected in
horizon B spodic of the profiles P2 and P5 (0.69-0.81 m and 0.87-0.98 m, respectively),
impregnated with a mixture of Polilyte polyester resin, styrene monomer, and fluorescent
pigment, using Butanox as a catalyst (de Castro et al., 2003), to prepare 30-µm fine sections.
The sections were observed using a polarizing optical microscopic (Carl Zeiss, Lab.A1 Axio,
Germany) and binocular magnifier (Carl Zeiss, 444036-9010, Germany), both under normal
and polarized light. Photomicrographs were obtained using a photomicroscopic camera (Carl

203	Zeiss, Axiocam 3	305 color,	Germany).	The	micromorphological	descriptions	followed	the
204	criteria and termin	nologies pro	oposed by B	ulloc	k et al. (1985) and Sto	pops (2003).		

From the morphological descriptions and analytical data (chemical and physical), soils were classified according to the World Reference Base for Soil Resources (IUSS Working Group WRB, 2015), in Podzols (profiles P1, P2, P3, P4 and P5) and Acrisols (P6).

208 3. Results and Discussion

209 **3.1. Morphological and physical attributes**

Soils described in both transects showed differences in terms of color, structure,
consistence, soil thickness, transition between horizons and physical attributes (Table 1).

212 Except for profile P6 that has a sequence of A-Btg horizons, the other profiles showed a spodic A-E-B sequence. In these profiles, underlying the E albic horizon, the spodic B 213 horizon appeared cemented in varying degrees, with a massive structure, characteristic of 214 ortstein, occurring with different thicknesses and at different depths (Fig. 2). Farmer et al. 215 216 (1983) indicate that this cementation occurs between the grains of quartz and organic compounds. In profiles P1, P2 and P3 the duric horizon occurs below the spodic B horizon 217 (Santos et al., 2015), a feature also observed by Oliveira et al. (2010) and Carvalho et al. 218 219 (2013) in Podzols of the Barreiras Formation in southern Bahia and Paraíba, respectively, northeastern Brazil. 220

This interpretation is also supported by GPR data (Fig. 2). The GPR1 line (Fig. 2) in the transect 1 (Fig. 1) reaches up to ~2.0 m thick and shows a distinct interface between the two contrasting materials with a lateral extension of several hundreds of meters (Fig. 2). At the top of the radargram, there are continuous sand medium amplitude and sub-horizontal reflections that extend from the top of the record to 1.5 m. These reflections could be related to the A and E horizon that resulted in a lower contrast in soil electrical properties and a 227 weaker GPR reflection, probably due to the process of the progressive illuviated silicate clays, with migration of clay-humus complexes to the underlying horizons. These conditions favor 228 the infiltration and drainage of rainwater for the B spodic horizon (Doolittle and Collins, 229 1995; Burgoa et al., 1991). On the radar record, the lower part of the A-E horizon is 230 characterized by a continuous strong reflection, showing a wavy or irregular geometry. This 231 reflection corresponds approximately to the top of the B spodic (1.5 m depth), i.e., below of 232 233 the spodic horizon, soil that contains silt or loamy particle-size classes with significant levels of moisture and organic carbon that can be related to genesis of duric horizon. The processes 234 associated with duric horizon formation result in hydro-consolidation that causes close 235 packing of grains and reduces porosity (Bockheim and Hartemink, 2013). The latter generates 236 a high radar signal associated with the presence of diagnostic subsurface horizons, 237 represented by a spodic horizon. Duric horizon has higher bulk densities and is less permeable 238 than overlying or underlying horizons (Doolittle et al., 2005), which can be significantly 239 attenuated by radar energy below the top of spodic horizons and no clear reflections were 240 detectable in the lower part of the radar record (Fig. 2; GPR1). 241

242 The GPR2 line (Fig. 2) obtained between P5 and P6 trenches (Fig. 1) reaches a depth of 3 m in the soil horizons, below which are weathered deposits of the Barreiras Formation 243 which extend to > 4 m. The high-amplitude interval lies around 1 m and shows a continuous 244 245 reflecting horizon, that can be coincident with the spodic horizon in P5 and/or Btg1 in P6. The top of the profile (Fig. 2) is dominated by discontinuous low amplitude, parallel to sub-246 horizontal reflections which appear to be related to the A horizon which is affected by water 247 infiltration, plant root penetration and undecomposed organic matter. These conditions favor 248 the occurrence of water in the near-surface layer (Mendonça et al., 2015), which can reflect a 249 250 discontinuity in the GPR signal at the top.

251 On the radargram GPR3 (Fig. 2) recorded at transect 2 (Fig. 1), the soil profile reaches 4 m, with great spatial variability in thickness (up to 6 m) and consists of three different 252 reflection patterns. The upper part, extending to 1.5 m, contains near horizontal internal 253 254 reflections with a strong amplitude signal and extends along the whole GPR profile. These stronger reflections signify a continuous A-E horizon and are interpreted as layers that contain 255 significant accumulations of silicate clay, organic matter and Fe and Al. Below this section, 256 257 down to 1 m, internal reflections change from subparallel to wavy with a concave shape and show a lateral extension of up to hundreds of meters with reflectors more segmented. While 258 the highest amplitudes are restricted to reflections in the depth range of 0.5 to 1 m, reflections 259 beneath were attenuated rapidly and are of low to very low amplitude (Fig. 2). These 260 reflectors are attributed to cemented spodic horizons and can be associated with the presence 261 of ortstein traced laterally on GPR lines. Cemented horizons are more compacted, with fewer 262 pores and differences in textural properties (Doolittle and Butnor, 2009; Afshar et al., 2017) 263 when compared to the overlapping layers and can generate high amplitude, and greater 264 attenuation of the GPR signal. As reported by Mokma et al (1990), the increased signal 265 266 reflections from the spodic horizon can produce high amplitude reflections that are associated with the presence of ortstein. The lowermost boundaries are imaged as high-amplitude and 267 268 contain subparallel to concave reflections and, lateral discontinuity, from which noises occur. This unconformity at a depth of around 4-5 m forms the lower boundary of the soil profile, 269 which can be attributed to weathered bedrock surfaces of the Barreiras Formation in situ. 270

The GPR data (Fig. 2) show that the top of the spodic horizons ranges in depth from about 0.6 to 2 m and developed in response to the process of reworking of weathered deposits of the Barreiras Formation, from which the radar energy was significantly attenuated, and no clear reflections are detectable. As reported by Doolittle and Butnor (2009), because of differences in their bulk density and water retention capacity, spodic horizons are detectablewith GPR.

Spodic horizons of profiles P1, P2, P3, P4 and P5 have a 10YR matrix with dark and 277 gray hues (low value and chroma), mainly due to the high content of organic matter, while in 278 albic E horizons, due to the multiple pedogenetic processes of translocation, whitish colors 279 were observed (high value). The presence of the E horizon is an indication of the pedogenetic 280 281 process of leucinization which creates a lighter coloured horizon (Kämpf and Curi, 2012). In general, these profiles have a structure ranging from granular to simple grains in A and E 282 horizons, and massive in the spodic B. Furthermore, the consistency of the surface horizons 283 was loose, while consistency of the spodic B horizons ranged from hard to extremely hard. In 284 general, all horizons had a wet non-plastic and non-sticky consistency. This characteristics of 285 soil consistency is a result of the coarse grain size in the horizons. Fine sand is predominant in 286 the profiles. The textural class ranges between sand, loamy sand, sandy loam and sandy clay 287 loam. 288

289 The differences in the depths of spodic B horizons, observed in the two areas studied, 290 is related to the oscillation of the water table, which is influenced by the altitude and shape of the relief (Santos et al., 2015; Coelho et al., 2010c). The GPR transect fluctuations of the 291 292 reflected signal in the radargram (Fig. 2) confirmed the variation in the depth of the spodic 293 horizon in the study areas. The largest dimensions occurred where the profile P1 is located, the level of the water table is far below the surface (> 1.0 m), and consequently, the top of the 294 spodic B horizon is formed from 1.43 m depth, and the albic E horizon is ~1.07 m thick. On 295 the other hand, for soils in micro-depressions, the water table occurs closer to the surface 296 (<1.0 m) for most of the year. In these cases, as noted in the profiles P2 and P5, the albic E 297 horizons range in thickness from 0.16 to 0.36 m and the spodic B are formed near the surface 298 (0.60 m). 299

300 The P6 profile has a 10YR hue in the superficial horizons, with low chroma and value, with colors ranging from dark gray brown to black. In sub-surface horizons the 2.5 Y hue is 301 predominant, with colors ranging from light grayish brown to light yellow brown. In this 302 303 profile, in superficial horizons, a granular-type structure occurs and in the sub superficial blocks, it was sub angular. A clay increment was observed with depth, with a textural gradient 304 of 1.8 associated with the textural class clay and clay loam. The increment of clay causes the 305 306 texture to be sticky and plastic when humid in the subsurface horizons of profile P6. In the GPR2 line the high reflection amplitudes up to 1m indicate abrupt changes in wave energy 307 which, can be attributed to an alternation in grain-size with the clay-rich B horizon. 308

It should be noted that in the subsurface horizons of the profiles, at a depth varying from 124 cm in profile P5 to 182 cm in P6, all material had a similar grain size, possibly as a result of the weathering in the Barreiras Formation.

312 **3.2.** Chemical attributes

The highest levels of TOC were observed in the surface horizons (horizon A and H) of all profiles, as well as in subsurface spodic B horizons of the profiles P1, P2, P3, P4 and P5, which is characteristic of the process of translocation of organic matter (Table 2). Depending on the sandy nature, the high levels of TOC influenced the sorption complex of the soils under study.

The pH values in water ranged from 3.8 on the Bhm2 horizon of profile P4, to 6.2 in the Bhx1 of profile P3, classified as extremely to moderately acidic, respectively (Santos et al., 2018). This pattern of high acidity of Podzols is related to the high values of H^+ and Al^{3+} present in the organic matter, mainly in the surface and subsurface spodic B horizons, corroborating other studies in sandbank areas (Gomes et al., 2007; Coelho et al., 2010c) and in the Barreiras Formation (Oliveira et al., 2010; Mafra et al., 2002, Silva et al., 2013; Carvalho et al., 2013). The highest levels of P occurred in subsurface horizons, with maximum values of 117 mg kg⁻¹, in the Bx2 horizon of the P2. Oliveira et al. (2010) observed high P content in Podzols of sandbank areas in the Barreiras Formation and that P is complexed with organic matter, being translocated in the profile and piling up on the spodic B due to the sandy soil texture. In addition, the reduction of crystallinity of iron oxides (Silva et al., 2013) by organic acids also explains the accumulation of P on the spodic B horizon.

In general the values of the exchangeable cations were low, K^+ was not detectable, and Na⁺, Ca²⁺ and Mg²⁺ ranged from 0 to 0.38, 0 to 2.1 and 0.1 to 2.9 cmol_c kg⁻¹, respectively, reflecting the low values of sum and bases saturation, characteristic of the Podzols category (Dias et al., 2003; Oliveira et al., 2010; Coelho et al., 2010 c; Mafra et al., 2002; Carvalho et al., 2013; Silva et al., 2013).

As with the total carbon content, the surface and B spodic horizons presented the 336 highest levels of Al^{3+} , H^+ and H + Al, suggesting that Al complex with organic material is 337 largely responsible for the genesis of the spodic B horizon (Van Breemen and Buurman, 338 1998). However, microbial degradation of organic compounds of the spodic B horizon can 339 promote the release and increase of exchangeable Al, as noted by Oliveira et al. (2010), in 340 agreement with the data of this study. Several studies have found high levels of Al^{3+} in the 341 342 spodic B horizon in different Podzol formation environments, such as sandbank areas (Coelho et al., 2010 c), the Barreiras Formation (Correa et al., 2008; Oliveira et al., 2010) and in the 343 North region (Mafra et al., 2002). 344

The forms of crystallinity of Fe and Al varied depending on the soils, as well as on depth in the profiles (Table 3). In the profiles P1, P2, P3, P4 and P5, besides the exchangeable Al, the Al content in oxalate extracts and DCB showed an accumulation of that element in spodic B horizons. The extracts of Fe oxalate and DCB showed low levels and did not vary with soil depth, suggesting greater participation of the Al complexed to the organic acids in the process of podzolisation, during the genesis of the spodic horizon (Coelho et al., 2010c; Oliveira et al., 2010). The Al/Fe ratios are high in both extracts, highlighting the relatively greater contribution of Al compared to Fe in the formation of the spodic B horizon. In addition, the Al_{0x}/Al_{DCB} ratio in subsurface horizons of all profiles studied was greater than the unit, indicative of the predominance of distinct forms of this element of lower crystallinity.

This pattern occurs as a result of the high levels of Al of the Barreiras Formation, as well as the hardening of the spodic horizon and the presence of duric horizon, that create an environment of water saturation, reducing and removing Fe from the system (Anderson et al., 1982; Corrêa et al., 2008; Coelho et al., 2010c; Oliveira et al., 2010; Carvalho et al., 2013; Silva et al., 2013). This process is intensified in soils of sandy texture, similar to those observed in the study area.

In the P6 profile, the Al levels were higher compared to Fe, both in DCB extracts and in oxalate, but without accumulation in specific horizons. The water table near the surface (~.1 m) provided a sharp build-up of organic matter and formation of subsurface Btg horizon with reductomorphic characteristics, with grayish colors typical of a reducing environment and removal of Fe (Santos et al., 2018), while Al was connected to the organic matter.

367 **3.3.** δ ¹³C and ¹⁴C ages of soil organic matter

The δ^{13} C of soil organic matter varied from -28.89 ‰ to -27.57 ‰ in profile P1, and -28.42 ‰ to -25.28 ‰ in the profile P4 (Fig. 3), characterizing the dominance of C₃ plants in both sites. These values are similar to those found in the modern dominant plants' species in the areas of profiles P1 (*Renvoizea trinii*) and P4 (*R. trinni* and *Lagenocarpus rigidus*), which are C₃ plants and present δ^{13} C of -28.9 ‰ and -28.4 ‰, respectively (Buso Junior et al., 2013). Enriched values of δ^{13} C observed in the B spodic horizons (P1 = -27.57‰; P4 = -25.28‰) may be related to the isotopic fractionation resulted from organic matter decomposition (Macko and Estep, 1984) and do not reflect changes in relative abundance of
C₃ and C₄ plants.

The ¹⁴C ages obtained from the humin in the B spodic horizons varied from 38,890 to 14,251 cal BP in profiles P1 and P4, respectively. Then, ¹⁴C ages and δ^{13} C values indicate that C₃ plants dominate the vegetation of the studied sites at least since the late Pleistocene.

Considering the organic matter in the B spodic horizon as a mixture of humin fractions 380 with different ages, the ¹⁴C ages obtained may reflect the minimum age, an aspect also 381 recorded by Perrin et al. (1964). They considered that in biologically inert B spodic horizons 382 of tropical oligotrophic Podzols, with low organic matter cycling, the ¹⁴C ages would reflect 383 the minimum age of formation of these horizons. Buurman and Jongmans (2005) argued that 384 oligotrophic Podzols in the tropical region, with reduced biologic activity, present longer 385 residence time of the organic matter in the B spodic horizon. Consequently, the difference in 386 the ages between P1 and P4 profiles would indicate differences in the time of formation of the 387 388 Podzols and/or in the vegetation covering in both sites. A similar situation was observed by Schwartz (1988) in Podzols in Congo, with ages varying from ~40,000 to 10,000 years BP. 389

In relation to environmental conditions that may lead to Podzol formation, Schwartz 390 (1988) related the ages of formation of spodic horizons with the time intervals of more humid 391 392 climates in Congo. Dubroeucq and Volkoff (1998) suggested that the process of Podzols formation in the Rio Negro basin would involve, in its initial stages, the acidic hydrolysis of 393 clay minerals by the soil solution. This initial process may be favored by higher 394 395 environmental humidity, consequently, the palaeoenvironmental conditions that led to the initial formation of the B spodic horizons were related to the time intervals of predominant 396 humid climates during late Pleistocene (at ~40,000 cal BP and ~14,000 cal BP). 397

Some palaeoenvironmental studies have suggested similar humid intervals for the 398 palaeoclimate in southeastern Brazil. Based on pollen analysis, Ledru et al. (1996), at Serra do 399 Salitre, Minas Gerais State, ~ 1200 km west of VNR, suggested high moisture levels during 400 the interval 40,000-27,000 BP (44,151-30,709 cal BP), with a maximum humidity at ~35,000 401 BP (40,095-38,843 cal BP). In the same study, the authors inferred the gradual increase in the 402 humidity after the late Glacial, during the interval 16,000 -11,000 BP (19,741-12,545 cal BP). 403 404 Pessenda et al. (2009), at the Curucutu Nature Reserve, São Paulo State, ~1000 km south of VNR, used pollen analysis in a peatland and C isotopes in the soil organic matter, to infer the 405 presence of a humid climate for the interval 28,000 - 15,000 BP (~31,500 - 18,000 cal BP), 406 characterizing the expansion of Araucaria forest in the region, today located ~500 km to the 407 south, at Paraná State. Veríssimo et al. (2012) studied a pollen record in the Serra do Caparaó, 408 ~230 km from VNR, and inferred humid climate for the transition Pleistocene - Holocene 409 (~11,500 cal BP). Based on δ^{18} O of stalagmites from south and southeastern Brazil, Cruz Jr et 410 al. (2005, 2006) suggested intervals of higher rainfall amounts around 45,000-40,000 411 (~48,000 - 43,000 cal BP) and 20,000-14,000 BP (~ 24,000 - 17,000 cal BP) in the Bt2 412 413 record, and around 47,000-37,000 (~ 50,000 - 40,000 cal BP) and 20,000-15,500 (~24,000 -18,500 cal BP) in the St8 record, caused by changes in the location and/or convective activity 414 415 of the South American summer monsoon.

416

6 **3.4. Micromorphology and genesis of soils**

The spodic horizons had similar micromorphological features (Table 4). Many areas observed in the thin sections had organic matter coatings completely filling the porous space, with a porphyric distribution pattern (Fig. 4c, 4e), a phenomenon already observed by Coelho et al. (2012) in spodic horizons formed in sandy materials from the coast of São Paulo state, Brazil. However, basic types of relative distribution such as chitonic, gefuric and enaulic can be observed in the thin sections of the spodic B horizons (Fig. 4a). The organic matter in the
spodic horizons, characterized by the advanced stage of transformation and absence of
cellular structures or original forms of vegetable remnants, can be identified as monomorphic
(De Coninck et al., 1974; Coelho et al., 2012).

In the studied horizons, there is a predominance of porosity cavity poly-concave, and the pores between the coarse grains of sub-rounded polycrystalline quartz (Fig. 4d) are filled with a fine organic matter of black tones in the central part and reddish at the extremities (Fig. 4e). This change in coloration evolves with the formation of channels and micro fissures (Fig. 4f), with subsequent separation of these constituents into smaller units, giving rise to complex microstructure with film bridges between grains and massive (Fig.4b).

In the study environment, the combination of factors such as excess moisture, 432 temperature and high acidity, sediment of the Barreiras Formation and flat relief, contribute to 433 the occurrence of the pedogenetic processes of ferrolysis (Dubroeucq and Volkoff, 1998; 434 Moreau et al., 2006) and podzolisation (Lundström et al., 2000; Corrêa et al., 2008; Oliveira 435 436 et al., 2010; Silva et al., 2013). In the area covered by forest vegetation (profile P6), one may 437 infer that these processes are largely responsible for the transformation of sedimentary material from the Barreiras Formation, with destruction of clays by the ferrolysis process. 438 439 This results in more sandy surface horizons followed by other clayey subsurface horizons and the formation of Acrisols. 440

In a lateral transformation sequence in Acrisols located in the higher parts of the study site, the ferrolysis at the top of the Bt horizon favored by the excess of moisture in this area of the profile, leads to the formation and thickening of the E horizon, at the expense of the Bt horizon (Mafra et al., 2002; Silva et al., 2013).

445 At a later stage, or simultaneously to the ferrolysis, the process of podzolisation takes 446 place, in which organic compounds such as dissolved humic and fulvic acids, complex and

remove metals, mainly Fe and Al, from the superficial horizons (A, H), translocating and 447 depositing them in the subsurface horizons and forming the spodic B (Mafra et al., 2002; 448 Oliveira et al., 2010; Silva et al., 2013). These processes can be noted in the profiles P1, P2, 449 P3, P4 and P5, located in the areas with grass vegetation, where there is a larger drainage 450 impediment layer. Oliveira et al. (2010) have pointed out that the Podzols of the Barreiras 451 Formation have a cemented spodic B horizon (Ortstein), which appears to have been formed 452 453 due to the lateral transport of silica and aluminum, related to the destruction of clays from the duric horizons of Acrisols and Ferralsols, located in the higher portions of the landscape, as 454 observed in the study area. In tropical conditions, which characterize our study, in sandy and 455 poorly drained soil, the spodic B horizon contains plenty of organic complexes and Al, but 456 little Fe oxides, which were reduced and removed by leaching. 457

The monomorphic predominance of the organic constituents evidences the 458 mobilization, illuviation and precipitation of the organic matter in the genesis of the spodic 459 horizon (De Coninck et al., 1974; De Coninck, 1980; Buurman et al., 2005; Coellho et al., 460 2012). The ¹⁴C ages indicate that the accumulation of organic material of C_3 plants from the 461 462 vegetation cover in B spodic horizons occurred since at least ~14,250 to 38,890 cal BP, in the profiles P4 and P1, respectively. These B horizons cause high-amplitude reflections in the 463 464 GPR data, indicative of abrupt changes in wave energy, that are attributed to the formation of a cemented or indurated soil, with orstein and duric horizon. 465

It is assumed that the genesis of the spodic horizons occurred in the past under accentuated hydromorphism (De Coninck, 1980; McKeague & Wang, 1980; Coellho et al., 2012). In Amazonian, the most waterlogged zones of the podzolized areas are the main source of dissolved organic matter, with an organic carbon accumulation rate in the Bh horizon of 0.54 to 3.17 g cm⁻² year⁻¹, which requires a long time for organic matter stabilization, whose ¹⁴C dating in the B spodic horizons ranged from 48,000 to 450,000 years BP (Doupoux, et al.,

2017). On the other hand, changes in the precipitation pattern, with greater frequency of dry 472 periods, resulting in less frequent waterlogging, decrease carbon flux to the Bh horizon 473 (Sierra et al., 2013), promoting instability and degradation of organic matter mainly at the top 474 475 of the B spodic horizon (Coelho et al., 2012). This hypothesis is supported by the fact that the differentiated coloration of organic matter in the voids is associated with different degrees of 476 decomposition, indicating differences in the chemical constituents of this organic material 477 478 (Buurman et al., 2005; Bardy et al., 2008). In an evolutionary stage of decomposition of the organic matter, the microfissures are formed, which evolve originating the voids space inter-479 grains of the cavity poly-concave type, initiating the process of destruction of the top B spodic 480 horizon. 481

482 **4.** Conclusions

The ground penetrating radar images showed that development of soil horizons occurs 483 directly over the weathered bedrock of the Barreiras Formation. The horizons in the top of 484 radargrams were differentiated by changes in the internal geometry of the reflectors and are 485 consistent with the findings of the soil pedons. The data also showed that spodic horizons in 486 transects 1 and 2 have variable thicknesses, which possibly correlate with podzolisation 487 processes, which reflect the lateral changes of the depth and degree of weathering of the 488 Barreiras Formation. The combination of a near-surface water table, humidity and excessive 489 acidity and sandy nature of the sediment of the Barreiras Formation, have favoured the 490 processes of ferrolysis and podzolisation. The destruction of clays and eluviation of organic 491 matter complexed with aluminum provided the genesis of Acrisols and Podzols, respectively. 492 493 The filling of the voids space by organic constituents evidences the process of illuviation of the organic matter, responsible for the genesis of the B spodic horizons. The accumulation of 494 organic compounds in the B spodic horizons of the P1 and P4 profiles originated from C3 495 plants, suggests the dominance of humid climate in the region since at least 38,890 cal BP. 496

497 Acknowledgments

To FUNDECT; to the CNPq/CAPES for the financial support through projects: "Casadinho" process 620029/20080 and "Casadinho/Procad" process 552377/2011-2; to CNPq (470210/2012-5, 302711/2013-9) and FAPESP (2007/03615-5, 2010/18091-4 and 2011/00995-7) for the financial support for the field trips and analyses.

502 **References**

- Afshar, A.F., Ayoubi, S., Castrignanò, A., Quarto, R., Ardekani, M. R. M., 2017. Using
 ground-penetrating radar to explore the cemented soil horizon in an arid region in Iran.
 Near Surface Geophysics, 15, 103-110.
- Anderson, H.A., Berrow, M.L., Farmer, V.C., Hepburn, A., Russel, J.D., Walker A.D., 1982.
 A reassessment of podzol formation processes. Journal of Soil Science, 33(1), 125-136.
- Bardy, M., Fritsch, E., Derenne, S. Allard, T., do Nascimento, N.R., Bueno, G.T. (2008).
 Micromorphology and spectroscopic characteristics of organic matter in waterlogged
 podzols of the upper Amazon basin. Catena, 145, 222-230.
- Bockheim, J.G., Hartemink, A. E., 2013. Soils with fragipans in the USA. Catena 104, 233242.
- 513 Boski, T., Angulo, R.J., Souza, M.C., Barboza, E.G., Knicker, H., González-Pérez, J.A.,
- González-Vila, F.J., 2015. Progradation rates of coastal barrier sands estimated from the
 14C age of soil organic matter. J. Quart. Sci. 30, 9–18.
- Bullock, P., Fedoroff, N., Jongerius, A., Stoops, G., Tursina, T., 1985. Handbook for Soil
 Thin Section Description. Waine Research Publications, Wolverhampton (152 pp).
- 518 Burgoa, B., Mansell, R.S., Sawka, G.J., Nkedi-Kizza, P., Capece, J., Campbell, K., 1991.

519 Spatial variability of depth to Bh horizon in Florida Haplaquods using ground-penetrating

radar. Soil and Crop Science Society of Florida Proceedings, 50, 125–130.

521	Buso Junior, A.A., Pessenda, L.C.R., De Oliveira, P.E., Giannini, P.C.F., Cohen, M.C.L.,
522	Volkmer-Ribeiro, C., Oliveira, S.M.B., Rossetti, D.F., Lorente, F.L., Borotti Filho, M.A.,
523	Schiavo, J.A., Bendassolli, J.A., França, M.C., Guimarães, J.T.F., Siqueira, G.S., 2013a.
524	Late Pleistocene and Holocene vegetation, climate dynamics, and Amazonian taxa in the
525	Atlantic Forest, Linhares, SE Brazil. Radiocarbon 55 (2-3), 1747-1762.
526	Buso Junior, A.A., Pessenda, L.C.R., Mayle, F.E., Lorente, F.L., Volkmer-Ribeiro, C.,
527	Schiavo, J.A.,., Pereira, M.G., Bendassolli, J.A., Macario, K.C.D., Siqueira, G.S. 2019.
528	Paleovegetation and paleoclimate dynamics during the last 7000 years in the Atlantic
529	Forest of Southeastern Brazil based on palynology of a waterlogged sandy soil. Review
530	of Palaeobotany and Palynology 264, 1–10.
531	Buurman, P.; Jongmans, A.G. 2005. Podzolisation and soil organic matter dynamics.
532	Geoderma 125, 71-83.
533	Buurman, P.; van Bergen, P.F.; Jongmans, A.G.; Meijer, E.L.; Duran, B., Van Lagen, B.
534	(2005). Spatial and temporal variation in podzol organic matter studied by pyrolysis-gas
535	chromatography/mass spectrometry and micromorphology. Eur. J. Soil Sci., 56:253-270.
536 537	Buurman, P., 1984. Podzols. Van Nostrand Reinhold Soil Science Series New York. (450 pp).
538	Buurman, P., Vidal-Torrado, P., Martins, V.M., 2013. The podzol hydrosequence of Itaguaré
539	(Sao Paolo, Brazil). 1. Geomorphology and interpretation of profile morphology. Soil
540	Sci. Soc. Am. J. 77, 1294–1306.
541	Calegari, M.R., Madella, M., Brustolin, L.T., Pessenda, L.C.R., Buso Júnior, A.A.,
542	Francisquini, M.I., Bendassolli, J.A., Vidal-Torrado, P., 2017. Potential of soil phytoliths,

- 543 organic matter and carbon isotopes for small-scale differentiation of tropical rainforest
- 544 vegetation: A pilot study from the campos nativos of the Atlantic Forest in Espírito Santo
- 545 State (Brazil). Quaternary International, 437, 156-164.

546	Carvalho, V.S., Ribeiro, M.R., Souza Júnior, V.S., Brilhante, S.A., 2013. Caracterização de
547	Espodossolos dos Estados da Paraíba e do Pernambuco, Nordeste do Brasil. Revista
548	Brasileira de Ciência do Solo, 37, 1454-1463.

- 549 Coelho, M.R., Martins, V.M., Vidal-Torrado, P., Souza, C.R.G., Perez, X.L.O., Vásquez,
- F.M., 2010 b. Relação solo-relevo-substrato geológico nas restingas da planície costeira
 do Estado de São Paulo. Revista Brasileira de Ciência do Solo, 34(2), 833-846.
- 552 Coelho, M.R., Vidal-Torrado, P., Perez, X.L.O., Martins, V.M., Vázquez, F.M., 2010c.
 553 Fracionamento do Al por técnicas de dissoluções seletivas em Espodossolos da planície

costeira do estado de São Paulo. Revista Brasileira de Ciência do Solo, 34(2), 1081-1092.

555

Coelho, M. R., Martins, V.M., Pérez, X.L.O., Vázquez, F.M., Gomes, F.H., Cooper, M.,

- Vidal-Torrado, P., 2012. Micromorfologia de horizontes Espódicos nas restingas do
 Estado de São Paulo. Revista Brasileira de Ciência do Solo, 36, 1380-1394.
- Corrêa, M.M., Ker, J.C., Barrón, V., Torrent, J., Fontes, M.P.F., Curi, N., 2008. Propriedades
 cristalográficas de caulinitas de solos do ambiente tabuleiros costeiros, Amazônia e
 Recôncavo Baiano. Revista Brasileira de Ciência do Solo, 32 (3), 1857-1872.
- 561 Cruz Jr, F.W., Burns, S.J., Karmann, I., Sharp, W.D., Vuille, M., Cardoso, A.O., Ferrari, J.A.,
- 562 Dias, P.L.S., Viana Jr, O., 2005. Insolation-driven changes in atmospheric circulation
 563 over the past 116,000 years in subtropical Brazil. Nature 434, 63-66.

Cruz Jr, F.W., Burns, S.J., Karmann, I., Sharp, W.D., Vuille, M., 2006. Reconstruction of
regional atmospheric circulation features during the late Pleistocene in subtropical Brazil
from oxygen isotope composition of speleothems. Earth and Planetary Science Letters
248, 495-507.

568	Dantas, J.S., Marques Júnior, J., Martins Filho, M.V., Resende, J.M.A., Camargo, L.A., &
569	Barbosa, R.S. (2014). Gênese de solos coesos do leste maranhense: relação solo-
570	paisagem. Revista Brasileira de Ciência do Solo, 38(3), 1039-1050.
571	de Castro, S.S., Cooper, M., Santos, M.C., Vidal-Torrado, P., de Lima, J.M., 2003.
572	Micromorfologia do solo: bases e aplicações. In: Curi, N., Marques, J.J., Guilherme,
573	L.R.G., Lopes, A.S., Alvarez Venegas, V.H. (Eds.), Tópicos em ciência do solo. Vol. 3.
574	Sociedade Brasileira de Ciência do Solo, Viçosa, MG, pp. 107–164.
575	De Coninck, F. 1980. Major mechanisms in formation of spodic horizons. Geoderma, 24:101-
576	126.
577	De Coninck, F.; Righi, D.; Maucorps, J., Robin, A.M. 1974. Origin and micromorphology
578	momenclature of organic matter in sandy spodosols. In: Rutheford, G.K., ed. Soil
579	microscopy. Ontario, Limestone Press. p.263-273.
580	Dias, H.C.T., Schaefer, C.E.G.R., Fernandes Filho, E.I., Oliveira, A.P., Michel, R.F.M.,
581	Lemos, J.B., 2003. Caracterização de solos Altimontanos em dois transectos no Parque
582	Estadual do Ibitipoca (MG). Revista Brasileira de Ciência do Solo, 27(2), 469-481.
583	Doolittle, J.A., Collins, M.E., 1995. Use of soil information to determine application of
584	ground-penetrating radar. Journal of Applied Geophysics 33, 101–108.
585	Doolittle, J.A., Butnor, J.R., 2009. Soils, peatlands and biomonitoring. In: Ground Penetrating
586	Radar: Theory and Applications (ed H.M. Jol), p. 179. Amsterdam, Netherlands:
587	Elsevier.
588	Doolittle, J., Daigle, J., Kelly, J., Tuttle, W., 2005. Using GPR to characterize plinthite and
589	ironstone layers in Ultisols. Soil Survey Horizons 46(4), 179–184.
590	Doupoux. C., Merdy, P., Montes, R.C., Nunan, N., Melfi, A.J., Pereira, O.J.R., Lucas, Y.,
591	2017. Modelling the genesis of equatorial podzols: age and implications for carbon

fluxes. Biogeosciences, 14 (1), 2429–2440.

593	Dubroeucq, D., Volkoff, B., 1998. From Oxisols to Spodosols and Histosols: evolution of the
594	soil mantles in the rio Negro basin (Amazonia). Catena, 32(1), 245-280.
595	Farmer, V.C., Russel, J.D., Smith, B.F.L., 1983. Extraction of inorganic forms of translocated
596	Al, Fe and Si from a Podzol Bs horizon. European Journal of Soil Science, 34(3), 571-
597	576.
598	Gomes, F.H., Vidal-Torrado, P., Macías-Vazquez, F., Gherardi, B., Otero, X.L., 2007. Solos
599	sob vegetação de restinga na Ilha do Cardoso-SP: I- Caracterização e classificação.
600	Revista Brasileira de Ciência do Solo, 31 (4), 1563-1580.
601	Hogg, A.G., Hua, Q., Blackwell, P.G., Niu, M., Buck, C.E., Guilderson, T.P., Heaton, T.J.,
602	Palmer, J.G., Reimer, P.J., Reimer, R.W., Turney, C.S.M., Zimmerman, S.R.H., 2013.
603	SHCal13 Southern Hemisphere calibration, 0-50,000 years cal BP. Radiocarbon 55 (4),

- 604 1889-1903.
- Horbe, A.M.C., Horbe, M.A. & Suguio, K. 2004. Tropical Spodosolsin northeastern
 Amazonas State, Brazil.Geoderma,119,55–68.
- IUSS Working Group WRB, 2015. World reference base for soil resources 2014, update
 2015. International soil classification system for naming soils and creating legends for
 soil maps. World Soil Resources Reports No. 106. FAO, Rome (1-192 pp.).
- 610 Kaczorek, D., Sommer, M., Andruschkewitsch, L., Oktaba, L., Czerwinski, Z., Stahr, K.,
- 611 2004. A comparative micrmorphological and chemical stydy of "Raseneisenstein"(bog
 612 iron ore) and "Orstein". Geoderma 121, 83–94.
- Kämpf, N., Curi, N. Formação e evolução do solo (Pedogênese). In: Ker, J.C., Curi, N.,
 Schaefer, C.E.G.R., Vidal Torrado, P., 2012. Pedologia: Fundamentos. (1ª ed.). Viçosa:
 SBCS, p.207-302.

616	Ledru, M-P., Braga, P.I.S., Soubiès, F., Fournier, M., Martin, L., Suguio, K., Turcq, B., 1996.
617	The last 50,000 years in the Neotropics (Southern Brazil): evolution of vegetation and
618	climate. Palaeogeography, Palaeoclimatology, Palaeoecology 123, 239-257.

- Lima Neto, J.A., Ribeiro, M.R., Corrêa, M.M., Souza Júnior, V.S., Lima, J.F.W.F., Ferreira,
- 620 R.F.A.L., 2009. Caracterização e gênese do caráter coeso em Latossolos Amarelos e
- Argissolos dos Tabuleiros Costeiros do Estado de Alagoas. Revista Brasileira de Ciência
 do Solo, 33(4), 1001-1011.
- Lopes-Mazzetto, J.M., Schellekens, J. Pablo Vidal-Torrado, P., Buurman, P. 2018. Impact of
 drainage and soil hydrology on sources and degradation of organic matter in tropical
 coastal podzols. Geoderma, 330, 79-90.
- 626 Lundstrom, U.S., van Breemen, N., Bain, D.C., van Hees, P.A.W., Giesler, R., Gustafsson,
- 527 J.P., Ilvesniemi, H., Karltun, E., Melkerud, P.A., Olsson, M., Riise, G., Wahlberg, O.,

Bergelin, A., Bishop, K., Finlay, R., Jongmans, A.G., Magnusson, T., Mannerkoski, H.,
Nordgren, A., Nyberg, L., Starr, M., Tau Srand, L., 2000a. Advances in understanding

- 630 the podzolization process resulting from a multidisciplinary study of three coniferous
- 631 forest soils in the Nordic Countries. Geoderma 94, 335–353.
- 632
- 633 Macario, K.D., Gomes, P.R.S., Anjos, R.M., Carvalho, C., Linares, R., Alves, E.Q., Oliveira,
- 634 F.M., Castro, M.D., Chanca, I.S., Silveira, M.F.M., Pessenda, L.C.R., Moraes, L.M.B.,
- 635 Campos, T.B., Cherkinsky, A, 2013. The Brazilian AMS radiocarbon laboratory (LAC-
- 636 UFF) and the intercomparison of results with CENA and UGAMS. Radiocarbon 55 (2-3),
 637 325-330.
- Mafra, A.L., Miklós, A.A.W., Volkoff, B., & Melfi, A.J. (2002). Pedogênese numa seqüência
 Latossolo-Espodossolo na região do alto rio negro, Amazonas. Revista Brasileira de
 Ciência do Solo, 26(2), 381-394.

641	Macko, S.A., Estep, M.L.F. (1984). Microbial alteration of stable nitrogen and carbon
642	isotopic compositions or organic matter. Organic Geochemistry, 6:787–90.
643	Martin, L., Suguio, K., Flexor, J.M., 1993. As flutuações do nível do mar durante o
644	Quaternario superior e a evolução de "deltas" brasileiros. Boletim IG-USP 15,
645	1e186.
646	Martinez, P., Lopes-Mazzeto, J.M., Buurman, P., Giannini, P.C.F., Schellekens, J., Vidal-
647	Torrado, P., 2018. Geomorphological control on podzolisation - An example from a
648	tropical barrier island. Geomorphology 309, 89–97.
649	Mckeague, J.A., Wang, C. (1980). Micromorphology and energy dispersive analysis of
650	orstein horizons of podzolic soils from New Brunswick and Nova Scotia, Canada. Can. J.
651	Soil Sci., 60:9-21, 1980.
652	Mckeague, J.A., Day, J.H., 1966. Dithionite-and oxalate-extractable Fe and Al as aids in
653	differentiating various classes of soils. Canadian Journal Soil Science, 1(1), 13-22.
654	Mehra, O.P., Jackson, M.L. 1960. Iron oxide removal from soils and clays by a dithionite-
655	citrate system buffered with sodium bicarbonate. Clays and Clay Minerals, 7(2), 317-27.
656	Mendonça, B.A.F., Fernandes Filho, E.I., Schaefer, C.E.G.R., Simas, F.N.B., de Paula, M.D.
657	2015. Os solos das Campinaranas na Amazônia brasileira: ecossistemas arenícolas
658	oligotróficos. Ciência Florestal, Santa Maria, 25 (4), 827-839.
659	Ministério do Meio Ambiente, 2000. Avaliação e Açõoes Prioritárias para a Conservação da
660	Biodiversidade da Mata Atlântica e Campos Sulinos. MMA/SBF,Brasília, p. 40.

- Montes, C.R., Lucas2, O. J. R. Pereira1, R. Achard2,*, M. Grimaldi2, and A. J. Melfi. Deep
 plant-derived carbon storage in Amazonian podzols. 2011. Biogeosciences, 8, 113–120.
- 663 Moreau, A.M.S.S., Ker, J.C., Costa, L.M., Gomes, F.H., 2006. Caracterização de solos de
- duas topossequências em Tabuleiros Costeiros do sul da Bahia. Revista Brasileira de
 Ciência do Solo, 30(4), 1007-1019.
- Mokma, D.L., Schaetzl, R.J., Doolittle, J.A., Johnson, E.P., 1990. Groundpenetrating radar
 study of ortstein continuity in some Michigan Haplaquods. Soil Sci Soc Am J 54:936–
 938.
- 669 Oliveira, A.P., Ker, J.C., Silva, I.R., Fontes, M.P.F., de Oliveira, A.P., Neves, A.T.G.R.,
- 2010. Spodosols pedogenesis under Barreiras formation and sandbank environments in
 the south of Bahia. Revista Brasileira de Ciência do Solo, 34(3), 847-860.
- Perrin, R.M.S., Willis, E.H., Hodge, C.A.H., 1964. Dating of humus podzols by residual
 radiocarbon activity. Nature 202(4928), 165-166.
- 674 Pessenda, L.C.R., Valencia, E.P.E., Camargo, P.B., Telles, E.C.C., Martinelli, L.A., Cerri,
- 675 C.C., Aravena, R., Rozanskj, K., 1996. Natural radiocarbon measurements in Brazilian
 676 soils developed on basic rocks. Radiocarbon 38(2), 203-208.
- 677 Pessenda, L.C.R., Buso Junior, A.A., Cohen, M.C.L., Calegari, M.R., Schiavo, J.A., França,
- 678 M., Lorente, F.L., Giannini, P.C.F., Oliveira, P.E., Rossetti, D.F., Siqueira, G.S.,
- 679 Francisquini, M.I., Volkmer-Ribeiro, C., Bendassolli, J.A., Madella, M., Osterrieth, M.,
- 680 Cechet, F.A., Felipe, P.L.L., Brustolin, L.T., Rasbold, G.G., Monteiro, M.R., 2015.
- 681 Estudos interdisciplinares da dinâmica da vegetação e marinha e inferências climáticas
- milenares e atuais na costa Norte do Espírito Santo. Ciência & Ambiente, 49(1), 181-206.
- 683 Pessenda L.C.R., De Oliveira, P.E., Mofatto, M., Medeiros, V.B., Garcia, R.J.F., Aravena, R.,
- Bendassoli, J.A., Leite, A.Z., Saad, A.R., Etchebehere, M.L., 2009. The evolution of a

- tropical rainforest/grassland mosaic in southeastern Brazil since 28,000 14C yr BP based
 on carbon isotopes and pollen records. Quaternary Research, 71, 437-452.
- Santos, H.G., Jacomine, P.K.T., Anjos, L.H.C., Oliveira, V.A., Lumbreras, J.F., Coelho,
 M.R., Almeida, J.A., Araújo Filho, J. C., Oliveira, J. B., Cunha, T.J.F. 2018. Sistema
 Brasileiro de Classificação de Solos. 5ª ed. revisada e ampliada. Brasília, DF: Embrapa,
 531p.
- Santos, R.D.; Santos, H.G.; Ker, J.C., Anjos, L.H.C.; Shimizu, S.H. 2015. Manual de
 descrição e coleta de solo no campo. 7.ed. Viçosa, MG, Sociedade Brasileira de Ciência
 do Solo/Embrapa Solos, 100p.
- Saporetti-Junior, A.W., Schaefer, C.E.R.; Souza, A.L., Soares, M.P., Araújo, D.S.D., MeiraNeto, J.A.A., 2012. Influence of soil physical properties on plants of the mussununga
 ecosystem, Brazil. Folia Geobotanica 47, 29-39.
- Sauer, D., Sponagel, H., Sommer, M., Giani, L., Jahn, R., Stahr, K., 2007. Podzol: soil of the
 year 2007. A review on its genesis, occurrence, and functions. J. Plant Nutr. Soil Sci. 170
- 699 (5):581–597. <u>https://doi.org/10.1002/jpln.200700135</u>.
- Schiavo, J.A., Dias Neto, A.H., Pereira, M.G., Rosset, J.S., Secretti, M.L., Pessenda, L.C.,
 2012. Characterization and classification of soils in the Taquari river basin Pantanal
 Region, State of Mato Grosso do Sul, Brazil. Revista Brasileira de Ciência do Solo,
 36(3), 697-707.
- Schwartz, D., 1988. Some podzols on Bateke sands and their origins, People's Republic of
 Congo. Geoderma 43, 229-247.
- Sierra, C.A., Jiménez, E.M., Reu, B., Peñuela, M.C., Thuille, A., Quesada, C.A., 2013. Low
 vertical transfer rates of carbono inferred from radiocarbon analysis in na Amazon
 Podzol. Biogeosciences, 10 (1), 3455–3464.

709	Silva, E.A., Gomes, J.B.V., Araújo Filho, J.C., Silva, C.A., de Carvalho, S.A, Curi, N., 2013.
710	Podzolização em solos de áreas de depressão de topo dos tabuleiros costeiros do Nordeste
711	Brasileiro. Revista Brasileira de Ciência do Solo, 37(1), 11-24.
712	Soil Survey Staff. Keys to soil taxonomy. 12th. ed. Washington, DC: USDA, Natural
713	Resources Conservation Service; 2014.
714	Stoops, G., 2003. Guidelines for Analysis and Description of Soil and Regolith Thin Sections.
715	Soil Science Society of America, Madison, Wisconsin.

- Stuiver, M., Reimer, P.J., 1993. Extended 14C database and revised CALIB 3.0 14C
 calibration program. Radiocarbon 35 (1), 215-230.
- Teixeira, P.C.; Donagemma, G.K.; Fontana, A.; Teixeira, W.G. 2017. Manual de métodos de
 análise de solo. Rio de Janeiro, 3ª ed. Revisada e ampliada Brasília, DF: Embrapa,
 573p.
- Ucha, J.M., Vilas Boas, G.S, Hadlich, G.M. 2010. O uso do radar de penetração no solo na
 investigação dos processos de transformação pedogeomorfológica. Revista Brasileira de
 Geomorfologia, 11 (1), 85-96.
- Van Breemen, N.V., Buurman, P., 1998. Soil formation. Dordrecht, Kluwer.
- Veríssimo, N., Safford, H.DF., Behling, H., 2012. Holocene vegetation and fire history of the
 Serra do Caparaó, SE Brazil. The Holocene 22(11), 1243-1250.
- 727 Yeomans, J.C., Bremner, J.M., 1988. A rapid and precise method for routine determination of
- organic carbon in soils. Communications Soil Science Plant Analysis, 19 (4), 1467-1476.

- 730
- 731
- 732
- 733

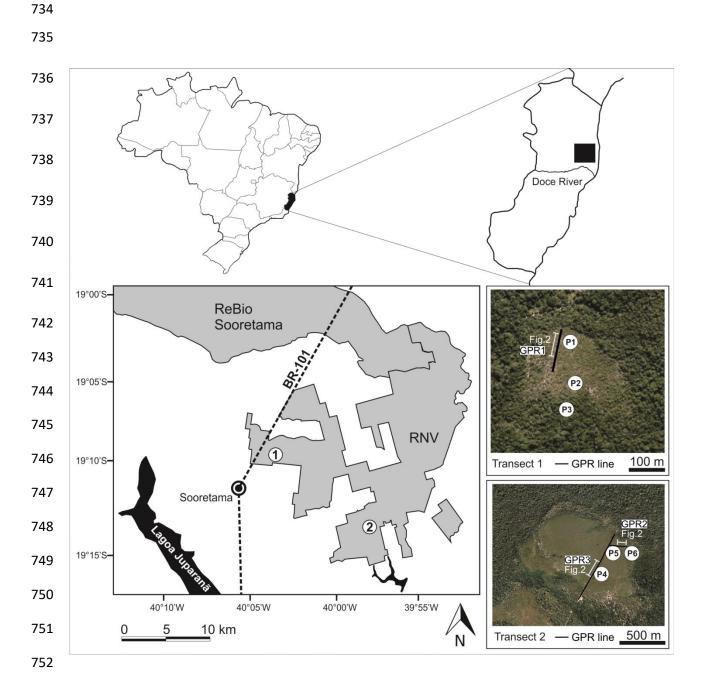
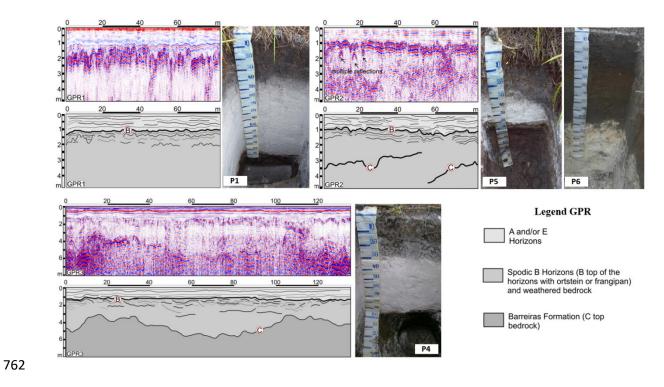


Figure 1. Study area map showing sampling locations and Ground penetrating radar (GPR)
activities in the forest grassland ecotone areas in the northeastern Espírrito Santo State, Brazil.
Transect 1 (profiles 1, 2 and 3) and Transect 2 (profiles 4, 5 and 6).



_ _ _ _

Figure 2. Ground penetrating radar (GPR) data and interpretation of the radargram with the
different soils horizons and deposits of the Barreira Formation identified in the profile.

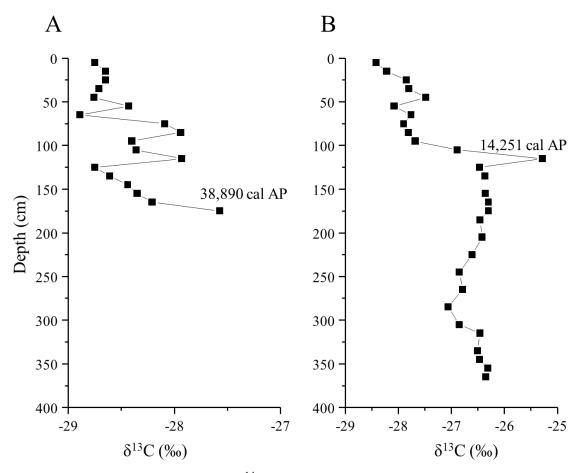


Figure 3. Variation of δ^{13} C (‰) and 14 C ages in profiles P1 (A) and P4 (B) of Podzols in the northeastern Espirito Santo State, Brazil.



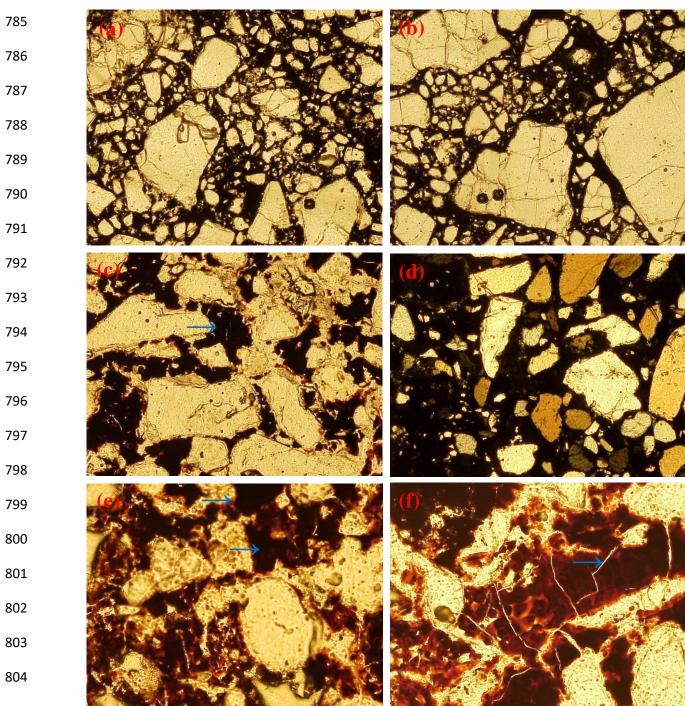


Figure 4. Photomicrographs in which can be observed: Horizon Bhm profile P2: (a) relative distribution chitonic-gefuric-porphyric; (b) complex pellicular microstructure with bridges and massive. Horizon Bh2 profile P5: (c) monomorphic organic matter completely filling the porosity (relative distribution $g/f_{2\mu m}$ porphyric); (d) coarse material, with quartz grains and porosity cavity poly-concave; (e) fine organic material filling the voids space, with dark coloration in the central part and reddish at the extremities; (f) presence of microfissures and dissolution of fine organic material.

- 813
- 814

Table 1. Morphological and granulomeric atributes of soils developed in the forest grassland

816 ecotone areas in the northeastern Espirito Santo State, Brazil.

Horizon	Depth	Munse	ell color	Structure ¹		onsisten		Transition ⁵	Sand	Clay	Silt	Texture class
	-	moist	dry	-	dry ²	moist ³	wet ⁴					
	m									-g kg ⁻¹		
				Tran	sect 1 - P	1 – gras	sland					
A1	0-0.18	10YR 3/1	10YR 4/1	we, sm/me, gr	sf	fb	np, ss	pc	982	4	14	Sand
A2	0.18-0.36	10YR 4/1	10YR 5/1	sg	1	ls	np, ns	pa	970	4	26	Sand
Е	0.36-1.43	10YR 8/1	10YR 8/1	sg	1	ls	np, ns	pa	945	2	53	Sand
Bhm1	1.43-1.49	10YR 3/1	10YR 5/2	massive	eh	ef	np, ns	pa	771	9	220	Loamy sand
Bhx1	1.49-1.60	10YR 3/1	10YR 4/2	mo, sm, ab	h	fb	np, ns	pa	683	23	294	Sandy loam
Bhx2	$1.60 - 1.74^+$	10YR 3/2	10YR 5/1	mo, sm, ab	h	fb	np, ns	-	668	29	303	Sandy loam
					P2-shr							
A1	0-0.15	10YR 3/1	10YR 4/1	we, sm/me, gr	sf	fb	np, ns	pc	845	10	145	Loamy sand
A2	0.15-0.25	10YR 4/1	10YR 5/1	sg	1	ls	np, ns	pa	922	7	71	Sand
E	0.25-0.61	10YR 8/1	10YR 8/1	sg	1	ls	np, ns	pa	919	71	10	Sand
Bhm	0.61-0.74	10YR 2/1	10YR 3/1	massive	h	fb	np, ns	pc	723	24	253	Loamy sand
Bx1	0.74-0.98	10YR 4/2	10YR 5/3	massive	vh	fb	np, ns	pc	692	31	277	Sandy loam
Bx2	$0.98 - 1.40^{+}$	10YR 5/3	10YR 6/3	massive	vh	fb	np, ns	-	757	157	86	Loamy sand
					P3 - wo	odland						
Н	0-0.12	2,5Y 2,5/1	2,5Y 3/1	mo,sm,gr	1	ls	np, ns	pc	885	77	38	Sand
A1	0.12-0.26	2,5Y 2,5/1	2,5Y 2,5/1	sg	1	ls	np, ns	pc	912	72	16	Sand
A2	0.26-0.40	2,5Y 4/1	2,5Y 5/1	sg	1	ls	np, ns	pc	940	53	7	Sand
E1	0.40-0.57	2,5Y 5/2	2,5Y 7/1	sg	1	ls	np, ns	pa	943	40	17	Sand
E2	0.57-1.34	2,5Y 7/1	2,5Y 8/1	sg	1	ls	np, ns	pa	918	56	26	Sand
Bhm	1.34-1.41	2,5Y 5/3	2,5Y 6/3	massive	eh	f	np, ns	pc	801	75	124	Loamy sand
Bhx1	1.41-1.49	10YR 4/2	2,5Y 5/2	massive	eh	ef	np, ns	pc	716	145	139	Loamy sand
Bhx2	1.49-1.69+	2,5Y 3/1	2,5 3/1	massive	h	vf	np, ns	-	657	293	50	Sandy clay loam
				Tran	sect 2 – P	4 – gras	sland					
A1	0-0.16	10YR 4/1	10YR 5/1	sg	1	ls	np, ns	pc	981	4	15	Sand
A2	0.16-0.22	10YR 4/1	10YR 5/1	sg	1	ls	np, ns	pc	970	4	26	Sand
E	0.22-0.91	10YR 8/1	10YR 8/1	sg	1	ls	np, ns	oa	945	2	53	Sand
Bhm1	0.91-0.93	10YR 4/1	10YR 5/2	massive	eh	vf	np, ss	pa	751	9	240	Loamy sand
Bhm2	0.93-1.11	10YR 3/1	10YR 3/2	massive	h	f	np, ss	pa	872	16	112	Sand
Bh	$1.11 - 1.28^+$	2,5Y 2,5/1	2,5Y 2,5/1	mo, sm, Bs	sf	fb	np, ns	-	610	36	354	Sandy loam
					P5 – shr	ubland						
A1	0-0.11	10YR 2/1	10YR 3/1	mo, me/l, gr	sf	fb	np, ns	pc	892	10	98	Sand
A2	0.11-0.34	10YR 3/1	10YR 4/1	sg	1	ls	np, ns	oc	924	8	68	Sand
E	0.34-0.60	10YR 7/1	10YR 8/1	sg	1	ls	np, ns	pa	916	8	76	Sand
Bhm	0.60-0.70	10YR 5/2	10YR 5/2	massive	eh	vf	np, ns	pc	711	12	277	Loamy sand
Bh1	0.70-0.87	10YR 2/1	10YR 3/1	mo, sm, ab	1	ls	np, ns	pc	545	45	410	Sandy loam
Bh2	0.87-1.15	10YR 3/2	10YR 4/2	mo, sm, ab	h	fb	np, ss	pc	748	23	229	Loamy sand
Bh3	$1.15 - 1.24^+$	10YR 3/2	10YR 4/2	mo, sm, ab	h	fb	np, ss	-	610	36	354	Sandy loam
					P6 – wo	odland						
A1	0-0.15	10YR 2/2	10YR 3/1	mo, sm, gr	sh	f	sp, ss	pc	774	183	43	Sandy loam
A2	0.15-0.34	10YR 2/1	10YR 3/2	mo, sm, gr	sh	f	sp, ss	pc	741	214	45	Sandy clay loam
A3	0.34-0.58	2,5Y 3/3	2,5Y 4/3	mo, sm, gr	h	f	np, ns	pc	708	262	30	Sandy clay loam
A4	0.58-0.73	2,5Y 3/2	2,5Y 5/3	mo, sm, sab	sh	fb	sp, ns	pc	732	246	22	Sandy clay loam
A5	0.73-1.00	2,5Y 3/2	2,5Y4/2	mo, sm, sab	sh	fb	sp, ns	pc	733	255	12	Sandy clay loam
Btg1	1.00-1.29	2,5Y 8/3	2,5Y 8/2	mo, sm, sab	h	f	p, s	pa	191	430	379	Clay
Btg2	1.29-1.50	2,5Y 8/3	2,5Y8/2	mo, sm, sab	h	f	p, s	pc	168	487	345	Clay
Btg3	$1.50 - 1.82^+$	2,5Y 8/3	2,5Y 8/2	mo, sm, sab	h	f	p, s	-	284	366	350	Clay loam

¹Structure: degree of development: (we: weak, mo: moderate), size (sm: small, me: medium, l: large), shape (gr: granular, sg: simple grains, ab: angular blocks, sab: subangular blocks). ²Dry consistence: (sf: soft, l: loose, eh: extremely hard, h: hard, vh: very hard, sh: slightly hard). ³Moist consistence: (fb: friable, ls: loose, ef: extremely firm, f: firm, vf: very friable). ⁴Wet consistence: (np: not plastic, p: plastic; sp: slightly plastic; ss: slightly sticky, ns: not sticky). ⁵Transition: (pc: plain and clear, pa: plain and abrupt, oa: ondulation and abrupt, oc: ondulation and clear).

824

⁸²³

Horizon	Depth	TOC	pH		Р	K^+	Na ⁺	Ca ²⁺	Mg^{2+}	H+A1	Al^{3+}	SB	Т	m	V
			Water	KCl	-				-						
	m	g kg ⁻¹			mg kg ⁻¹				-cmol	• kg-1					%
					Transect	1 - P	1 – gras	sland							
A1	0-0.18	14.5	4.4	2.6	7	0	0.09	0.9	0.3	11.3	1.7	1.3	12.6	14	10
A2	0.18-0.36	16.7	4.4	2.7	12	0	0.01	1.0	0.2	5.6	1.3	1.2	6.8	19	18
Е	0.36-1.43	3.7	5.3	4.3	1	0	0.01	0.3	0.1	0.4	0.1	0.4	0.8	12	5
Bhm1	1.43-1.49	19.0	4.0	2.8	2	0	0.01	0.2	0.2	17.8	4.5	0.4	18.2	25	2
Bhx1	1.49-1.60	26.5	4.1	3.4	33	0	0.01	0.3	0.1	33.2	4.5	0.4	33.6	13	1
Bhx2	$1.60 - 1.74^+$	30.5	4.2	3.6	28	0	0.01	0.3	0.1	15.0	3.1	0.4	15.4	20	3
					P2		ıbland								
A1	0-0.15	14.5	4.3	2.4	13	0	0.23	2.1	1.0	26.4	2.1	3.3	29.7	7	11
A2	0.15-0.25	5.2	4.3	2.6	18	0	0.02	0.7	0.2	6.9	1.2	0.9	7.8	15	12
Е	0.25-0.61	5.0	5.1	3.7	0	0	0.01	0.3	0.1	0.2	0.1	0.4	0.6	16	6
Bhm	0.61-0.74	27.5	4.0	3.0	8	0	0.06	0.4	0.1	35.9	8.6	0.6	36.5	24	2
Bx1	0.74-0.98	8.2	4.1	3.6	26	0	0.38	0.1	0.1	15.1	5.1	0.6	15.7	33	4
Bx2	$0.98 - 1.40^+$	9.2	4.3	3,7	117	0	0.37	0.0	0.1	14.3	3.2	0.5	14.8	22	3
							odland								
Н	0-0.12	92.3	4.1	2.8	21	0	0.39	0.4	2.9	22.6	4.7	3.3	25.9	41	13
A1	0.12-0.26	45.5	4.5	2.9	9	0	0	0.3	1.0	10.7	2.2	1.3	12.0	37	1
A2	0.26-0.40	21.3	4.5	3.2	9	0	0	0.4	0.2	7.6	1.5	0.6	8.2	29	7
E1	0.40-0.57	9.6	5.8	3.6	5	0	0	0.2	0.1	4.8	0.5	0.3	5.1	38	6
E2	0.57-1.34	7.0	6.0	4.6	3	0	0	0.3	0.2	4.9	0.3	0.5	5.4	63	9
Bhm	1.34-1.41	15.8	6.1	4.0	4	0	0	0.2	0.8	5.4	0.6	1.0	6.4	63	10
Bhx1	1.41-1.49	15.2	6.2	3.8	6	0	0	0.1	0.7	10.0	3.3	0.8	10.8	20	7
Bhx2	1.49-1.69+	61.0	6.1	4.0	23	0	0	0.3	0.2	19.6	6.7	0.5	20.1	7	2
					Transect	2 – P	-	ssland							
A1	0-0.16	8.0	4.2	2.7	5	0	0.01	0.5	0.2	5.5	0.9	0.7	6.2	14	11
A2	0.16-0.22	2.3	4.5	2.9	5	0	0.01	0.8	0.3	3.3	0.6	1.1	4.4	14	2
Е	0.22-0.91	1.8	5.2	4.4	0	0	0.02	0.5	0.2	1.2	0.2	0.7	1.9	10	31
Bhm1	0.91-0.93	7.2	4.2	2.8	0	0	0.01	0.3	0.1	10.8	1.5	0.4	11.2	13	4
Bhm2	0.93-1.11	35.2	3.8	2.6	0	0	0.01	0.5	0.3	56.2	7.6	0.8	57.0	13	1
Bh	$1.11 - 1.28^+$	33.9	3.9	2.8	2	0	0.01	1.0	0.4	49.6	5.8	1.4	51.0	11	3
							ubland								
A1	0-0.11	6.3	3.9	2.6	11	0	0.16	0.9	0.3	16.2	2.5	1.4	17.6	14	8
A2	0.11-0.34	9.3	4.1	2.7	6	0	0.02	0.3	0.2	6.5	1.5	0.5	7.0	21	7
Е	0.34-0.60	2.0	4.7	4.0	0	0	0.02	0.5	0.2	0.2	0.2	0.7	0.9	22	78
Bhm	0.60-0.70	22.5	4.2	3.2	1	0	0.02	0.2	0.1	10.6	2.9	0.3	10.9	27	3
Bh1	0.70-0.87	14.5	4.4	3.3	14	0	0.01	0.2	0.1	30.3	5.9	0.3	30.6	19	1
Bh2	0.87-1.15	18.2	4.4	3.8	29	0	0.01	0.1	0.1	12.4	2.5	0.2	12.6	20	2
Bh3	$1.15 - 1.24^+$	25.5	4.3	3.7	13	0	0.01	0.3	0.1	11.9	3.1	0.4	12.3	25	3
							odland								
A1	0-0.15	58.5	4.5	3.6	13	0	0.14	0.3	0.1	12.1	2.5	0.4	12.5	14	3
A2	0.15-0.34	38.1	4.7	3.8	11	0	0.32	0.4	0.3	15.0	2.4	0.7	15.7	23	4
A3	0.34-0.58	58.8	4.9	4.1	8	0	0.12	0.3	0.1	24.0	3.0	0.4	24.8	12	2
A4	0.58-0.73	48.7	5.0	4.2	6	0	0.12	0.3	0.1	18.2	1.9	0.4	18.6	17	2
A5	0.73-1.00	37.0	5.0	4.3	6	0	0.14	0.3	0.1	14.5	1.8	0.4	14.9	18	3
Btg1	1.00-1.29	16.4	5.0	4,1	4	0	0.08	0.3	0.2	8.0	1.7	0.5	8.5	23	6
Btg2	1.29-1.50	17.2	5.0	4.2	4	0	0.00	0.3	0.2	6.6	2.0	0.5	7.1	20	7
Btg3	$1.50 - 1.82^+$	21.1	4.9	4.1	5 Veoman	0	0.06	0.3	0.1	6.0	1.5	0.4	6.4	21	6

Table 2. Chemical attributes of soils developed in the forest grassland ecotone areas in thenortheastern Espirito Santo State, Brazil.

TOC: total organic carbono (method of Yeomans e Bremner); pH em água e KCl (1:2,5); P, K e Na:
extracted by Mehlich-1; Ca, Mg e Al: extracted by KCl 1 mol L⁻¹; H+Al: extracted by calcium acetate

830 $0.5 \text{ mol } L^{-1} \text{ pH } 7.0$; SB: bases of sum; m: saturation by aluminum; V: saturation by bases.

832	Table 3. Fe e Al extracted by oxalate (Ox) and dithionite-citrate-bicarbonate (DCB) and the
833	ratio of these metals of soils developed in the forest grassland ecotone areas in the
834	northeastern Espirito Santo State, Brazil.

Horizon	Depth		Oxala			DCB		Alox/Aldcb	Feox/FeDC
TIOTIZOII	Deptii	Al	Fe	Al/Fe	Al	Fe	Al/Fe	Alox ADCB	TCox/TCDC
	m	−g kg	g ⁻¹		—g k	g ⁻¹			
				nsect 1 -					.
A1	0-0.18	0.02	0.02	0.68	0.00	0.48	0.00	0.00	0.05
A2	0.18-0.36	0.00	0.01	0.00	0.00	0.45	0.00	0.00	0.02
Е	0.36-1.43	0.00	0.00	0.00	0.00	0.58	0.00	0.00	0.01
Bhm1	1.43-1.49	0.90	0.01	87.94	0.62	0.52	1.21	1.44	0.02
Bhx1	1.49-1.60	3.38	0.01	413.47	4.06	0.52	7.77	0.83	0.02
Bhx2	1.60-1.74+	2.59	0.04	58.59	1.71	0.47	3.68	1.51	0.09
4.1	0.0.15	0.16	0.04		rublan		0.04	4.07	0.04
A1	0-0.15	0.16	0.04	4.04	0.04	0.95	0.04	4.07	0.04
A2	0.15-0.25	0.03	0.02	1.48	0.00	0.87	0.00	0.00	0.02
E	0.25-0.61	0.00	0.01	0.00	0.00	0.83	0.00	0.00	0.01
Bhm	0.61-0.74	3.78	0.05	69.51	4.29	0.90	4.78	0.88	0.06
Bx1	0.74-0.98	2.89	0.02	117.26	1.91	0.73	2.61	1.51	0.03
Bx2	0.98-1.40+	5.26	0.03	167.68	3.49	0.88	3.96	1.51	0.04
	0.0.10	0.00	0.04		odland		0.50	0.07	0.00
Н	0-0.12	0.02	0.04	0.43	0.27	0.47	0.58	0.07	0.09
A1	0.12-0.26	0.02	0.01	1.44	0.23	0.53	0.45	0.09	0.03
A2	0.26-0.40	0.01	0.01	0.95	0.18	0.47	0.38	0.05	0.02
E1	0.40-0.57	0.00	0.00	0.41	0.13	0.39	0.35	0.01	0.01
E2	0.57-1.34	0.00	0.00	0.25	0.29	0.49	0.59	0.00	0.01
Bhm	1.34-1.41	0.05	0.04	1.09	0.56	0.56	1.00	0.08	0.08
Bhx1	1.41-1.49	0.99	0.05	17.99	1.14	0.45	2.55	0.87	0.12
Bhx2	1.49-1.69+	6.24	0.19	33.33	3.85	0.40	9.55	1.62	0.46
A 1	0.0.16	0.00		nsect 2 –				0.00	0.05
A1	0-0.16	0.00	0.02	0.00	0.00	0.42	0.00	0.00	0.05
A2	0.16-0.22	0.00	0.01	0.00	0.00	0.56	0.00	0.00	0.02
E Dhara 1	0.22-0.91	0.00	0.00	0.00	0.00	0.55	0.00	0.00	0.01
Bhm1	0.91-0.93	0.49	0.03	15.88	0.28	0.46	0.61	1.76	0.07
Bhm2	0.93-1.11	3.48 3.28	0.01 0.01	241.19	3.48 3.65	0.51	6.88	1.00	0.03
Bh	1.11-1.28+	5.28	0.01	247.33		0.61	6.03	0.90	0.02
A 1	0.0.11	0.08	0.10	P5 - sh	0.00		0.00	0.00	0.15
A1 A2	0-0.11 0.11-0.34	$\begin{array}{c} 0.08 \\ 0.05 \end{array}$	0.10 0.04	0.82 1.17	0.00	0.68 0.43	$\begin{array}{c} 0.00 \\ 0.00 \end{array}$	0.00 0.00	0.15 0.10
A2 E	0.11-0.34	0.00	0.04	0.00	0.00	0.43	0.00	0.00	0.10
ь Bhm	0.54-0.60	0.00	0.01	23.81	0.00	0.41	1.50	0.00	0.01
Bhli Bhl	0.70-0.87	4.85	0.03	129.02	5.70	0.50	11.43	0.91	0.00
Bh1 Bh2	0.70-0.87	4.85	0.04	129.02	2.37	0.30	3.19	0.83	0.08
Bh2 Bh3	1.15-1.24+	1.77	0.02	76.26	1.51	0.67	2.26	1.17	0.02
DIIS	1.15-1.24	1.//	0.02	P6 – w			2.20	1.17	0.05
A1	0-0.15	1.15	0.22	5.15	1.50	u 0.66	2.27	0.77	0.34
A2	0.15-0.34	2.40	0.15	16.49	1.90	0.00	3.97	1.26	0.30
A3	0.34-0.58	18.23	0.62	29.44	15.48	0.70	21.97	1.18	0.88
A4	0.58-0.73	11.25	0.02	33.34	11.02	0.67	16.37	1.02	0.50
A5	0.73-1.00	8.57	0.14	61.95	7.12	0.45	15.68	1.20	0.30
Btg1	1.00-1.29	5.13	0.57	9.05	3.44	0.45	4.09	1.49	0.68
Btg2	1.29-1.50	3.56	0.42	8.39	2.47	0.78	3.16	1.44	0.54
Btg3	1.50-1.82 ⁺	3.34	0.42	10.88	2.39	0.65	3.67	1.40	0.47

Table 4. Main micromorphological characteristics of the subsurface horizons of soils
developed in the forest grassland ecotone areas in the northeastern Espirito Santo State,
Brazil.

	Transect 1. Profile P2- grasses. Bhm - Bx1. 0.61-	Transect 2. Profile P5- grasses. Bh2. 0.87-1.15
	0.98 m.	m.
Matrix	Coarse material: 65%	Coarse material: 50%
	Fine material: 20%	Fine material: 35%
	Porosity: 15%	Porosity: 15%
Relative distribution	Complex: chitonic-gefuric-porphyric.	Complex: porphyric-enaulic.
Coarse material	Composed of polycrystalline quartz grains, sub- rounded, subangular, smooth/wavy, sub sphere and poorly selected. Frequency: dominant (60- 70%).	Composed of polycrystalline quartz grains, sub- rounded, subangular, smooth/wavy, sub sphere and poorly selected. Frequency: dominant (60- 70%).
Fine material	Predominantly organic matter and clay	Clay, iron oxide and mainly organic matter.
Pores	Porosity cavity, poly-concave, with irregular cavities, channels, fissures and microfissures. Presence of some stacking pores	Porosity cavity, poly-concave, stacking. Some channels and microfissures in the fine material.
Microstructure	Complex: Film (organic matter and clay) with bridges and massive.	Complex: polyhedral microgranular aggregates with presence of coalesced zones forming a dense mass
Birefringent fabric	Undifferentiated	Undifferentiated
Pedological features	Grains covered by cutans of organic material.	Grains covered by cutans of organic material.
842		
843		
844		
845		